RESEARCH PAPER

Rotational regimes of freely suspended liquid crystal films under electric current in presence of an external electric field

R. Shirsavar · A. Amjadi · M. R. Ejtehadi · M. R. Mozaffari · M. S. Feiz

Abstract The electrohydrodynamic (EHD) vortices produced by an electric current in freely suspended liquid crystal (LC) films of N-(4-methoxybenzylidene)-4-butyl-aniline (MBBA), convert to a pure rotation in the presence of external electric field (E_{ext}) perpendicular to the current direction. Here, the direction and strength of the rotation are precisely under control by our self-made device called "liquid-film motor". In this paper, we present experimental observations of the EHD fluid flow when external electric field varies from zero to a value in which pure rotation on the liquid crystal (LC) film is observed. We also show experimentally that the presence of external electric field causes a great decrease in the current produced by the voltage V_J required for observing EHD vortices in freely suspended films of MBBA. The LC films begin to rotate when E_{ext} V_J reaches a threshold value. This threshold is investigated experimentally as a function of voltage V_J and the external electrical field E_{ext}.

R. Shirsavar · A. Amjadi · M. R. Ejtehadi · M. S. Feiz (✉)
Department of Physics, Sharif University of Technology,
P.O. Box 11155-9161, Tehran, Iran
e-mail: sadegh.feiz@gmail.com

R. Shirsavar
e-mail: shirsavar@physics.sharif.edu

A. Amjadi
e-mail: amjadi@sharif.edu

M. R. Ejtehadi
e-mail: ejtehadi@sharif.edu

M. R. Mozaffari
Department of Physics, Qom University,
P.O. Box 3716146611, Qom, Iran
e-mail: m.mozaffari@qom.ac.ir

1 Introduction

Suspended liquid films thin as hundreds of nanometers or less allow us to study physical phenomena in a quasi-two-dimensional medium (Couder et al. 1989; Chomaz and Cathalau 1990; Rivera and Wu 2000; Huang et al. 2004). Applying an electric field can produce electro-hydrodynamical (EHD) flow in the liquid films, a topic which has been studied widely (de Gennes and Prost 1995; Chandrasekhar 1992; Sonin 1998). These works are important because manipulations of rotation have many applications as in micro-motors or drug delivery devices (*lab-on-a-chip*).

Electric field can produce instabilities in non-polar (Atten 1996; Saville 1997; Lee et al. 2000; Lee and Kang 1999; Collins et al. 2008) and polar (Ramos et al. 1998, 1999) liquids. The effect of electric field on liquid crystal (LC) films have been studied widely. Mostly, the electric field have been applied on LC films confined between two conductive transparent plates (de Gennes and Prost 1995; Chandrasekhar 1992; Xie et al. 2010a, b, 2011). On such confined LC films sufficiently large electric fields can produce electrohydrodynamic (EHD) instabilities, such as Williams domains and Chevrons Sonin (1998). Due to the friction between the liquid and the substrates at the boundaries, EHD instabilities in confined films are difficult to measure. Faetti et al. (1983a, b) have studied EHD instabilities on freely suspended films of nematic LCs that were not confined by any plate or substrate. They have reported a domain mode (Faetti et al. 1983a) for MBBA films with thickness of about 10 μm and a vortex mode (Faetti et al. 1983b) for thinner films.

The vortex mode is a line of vortices in which nearest-neighbour vortices have opposite senses of rotation. To produce the vortex mode, a minimum voltage is necessary to build up the required electric current passing through the film. This voltage is called the threshold voltage (Sonin 1998). Electro-convection in a suspended LC film of octylcyanobiphenyl (8 CB); that is in smectic A phase at room temperature, under large enough potential difference was investigated by Deyirmenjian et al. (1997). In all of these studies, induced electric charges on the surface of the film are known to be responsible for the vortex mode formation (Faetti et al. 1983b; Morris et al. 1990; Sonin 1998)

We have recently shown that in addition to the current passing through the film, by applying an external electric field $\mathbf{E}_{ext}$ perpendicular to and in the plane of the electric current, one can manipulate and control the direction and the velocity of rotation in suspended films of water (Amjadi et al. 2009) and other is increased up to polar liquids (Shirsavar et al. 2011). The sense of rotation depends on the direction of both the electric current and the external electric field, i.e. $\mathbf{E}_{ext} \times \mathbf{J}$ (Amjadi et al. 2009). Moreover, the velocity of the rotation depends on the strength of both the electric voltage V_J and the external electric field (Shirsavar et al. 2011) $\mathbf{E}_{ext}$. In reference, Amjadi et al. (2009), we have reported that reaching the pure rotation mode, both the electric voltage V_J which produces the electric current, and the applied electric field $\mathbf{E}_{ext}$ are important (Amjadi et al. 2009). We have also shown that in addition to water films, many other polar liquid films rotate when sufficiently large electric voltage and external field are applied (Shirsavar et al. 2011). The rotational motion of a dielectric liquid under $\mathbf{E}_{ext}$ has been also investigated (Grosu and Bologa 2010). The dynamic mechanism of a "liquid film motor" has been studied theoretically recently by Grosu and Bologa (2010), Shiryaeva et al. (2009), Liu et al. (2011).

In this article, following the references Faetti et al. (1983b), Morris et al. (1990), we study freely suspended LC films of MBBA in a rectangular and circular frame made of fiberglass with a pair of coated graphite electrodes on the opposite sides of the frame (Figs. 1, 2a). By placing the device at the center of a large capacitor with parallel plates, an electric field $\mathbf{E}_{ext}$ is applied on the film plane, perpendicular to the direction of V_J gradient. The geometry of the frame has no influence on physics of the problem and for simplicity of investigation, different geometries have been constructed and used.

Here, we shall experimentally demonstrate that external field can control transition from vortex mode to a single rotation (the sense of rotation is determined by $\mathbf{E}_{ext} \times \mathbf{J}$).
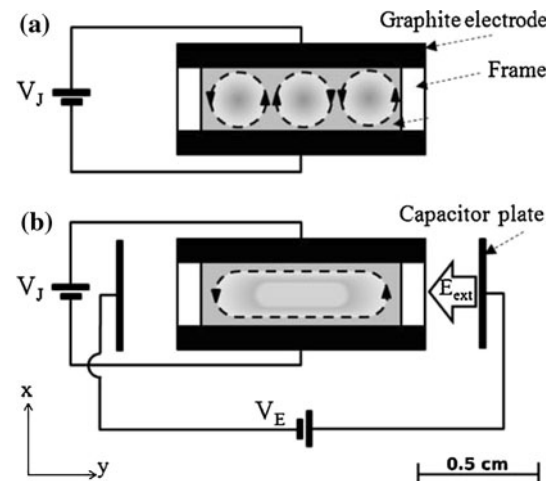

Fig. 1 Set-up of the experiment: a rectangular insulating frame with coated graphite electrodes on its *upper* and *lower* sides. **a** When the applied electric voltage V_J is sufficiently large, some vortices will be produced on the films. **b** By applying a large enough external electric field E_{ext} on the film, the vortices convert to a single pure rotation

2 Material and methods

2.1 Material

We use N-(4-Methoxybenzylidene)-4-butylaniline (MBBA) liquid crystal with 98% purity purchased from Aldrich. MBBA is in nematic phase at room temperature, and it has a phase transition from nematic to isotropic phase at 40.6°C. To control the phase of MBBA film, we use an IR light source to rise the film temperature, which is measured by an IR thermometer (TES-1326S). The IR radiation is focused on the film uniformly, and increases it is temperature from room temperature to above 40.6°C and therefore, MBBA film goes from nematic to isotropic phase.

2.2 Particle image velocimetry

Particle image velocimetery (PIV) (Shirsavar et al. 2011) is employed for velocimetry of suspended films rotation. At room temperature, MBBA is a viscous liquid and its film thickness decreases slowly. When the film is drawn it is much thicker than the coherence length of the exposed white light. Consequently, interference color patterns of white light cannot be observed. To detect the rotation, tracer particles, such as gold or aluminium flakes smaller than 50 μm were added to the film and its rotation were recorded by a high-speed camera (Casio EX-F1) at the rate of 300 frames per second. For each measurement, we have taken 100 consecutive images with a time separation of 3.3 ms.[1]

---

[1] Movies are available from http://www.softmatter.cscm.ir/Film Motor.

Fig. 2 Rotation in a circular frame. **a** A circular frame set-up, **b** a rotating liquid crystal film with particles as tracers on the MBBA film in circular frame with radius 3.5 mm, **c** angular velocity vector field when $E_{ext} = 300$ kV/m and $V_J = 2.3$ kV, **d** normalized velocity versus normalized radius, for MBBA (LC) film at $E = 300$ kV/m and $V_J = 2.3$ kV
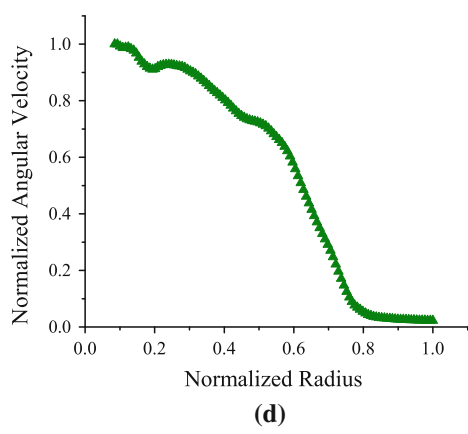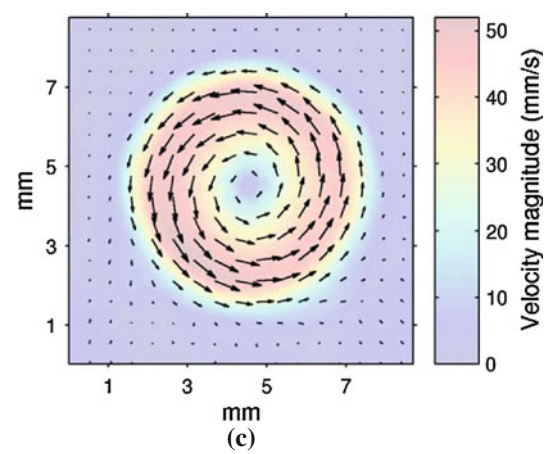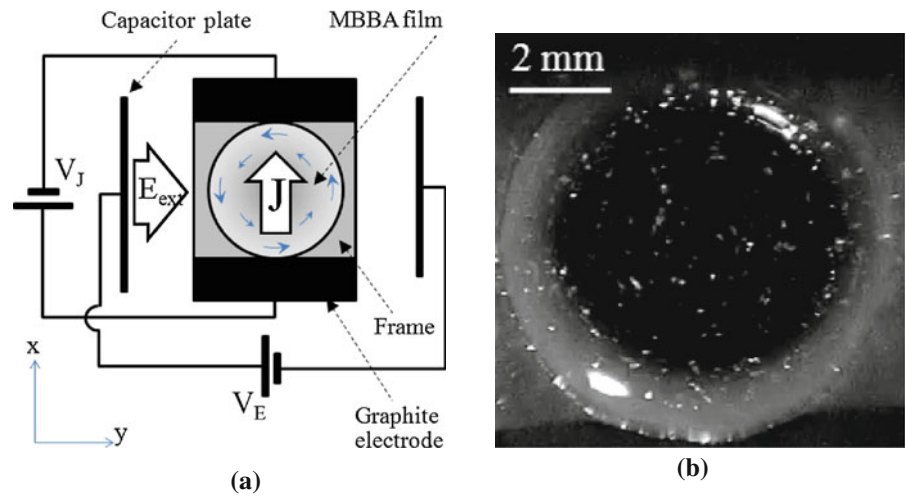
3 Experiment

3.1 Experimental procedures

Figure 1 shows the geometry of the rectangular frame (5 × 14 mm) that is placed horizontally inside the capacitor. The MBBA film is spread by a brush on the frame with size of $L_x = 3$ mm and $L_y = 10$ mm. A power supply applies V_J to produce a current density **J** in x-direction through the film, and another power supply charges the capacitor to apply external electric field $\mathbf{E}_{ext}$ in y-direction. The film thickness after the fluctuation became <7 μm (Faetti et al. 1983b). We have not measured the film thickness experimentally, but if the liquid crystal film thickness falls below a critical value, the reflected beams from the front and back surfaces of the film have 180°

phase shift. Therefore, it could not be observed, and the film looks black. In our experiment, after spreading the film on the frame, we wait a few minutes until MBBA film reaches its equilibrium state. Then the power supply V_J is turned on and the voltage is increased up to 900 V so that electrohydrodynamical vortex mode is observed (Fig. 3a). The next step is to apply the external electric field. By increasing the E_{ext}, we observe that the clockwise vortices expand and counterclockwise ones shrink (Fig. 3b–d). We have to mention that in our set-up the direction of $E_{ext} \times J$ is clockwise. Finally, by increasing the electric field up to about 500 kV/m, a single clockwise rotation mode on MBBA film (Fig. 3e) is obtained. Rotation direction obeys $\mathbf{E}_{ext} \times \mathbf{J}$ rule, which is reported in reference (Amjadi et al. 2009). In other words, by applying the electric field, the size of vortices which rotate in $\mathbf{E}_{ext} \times \mathbf{J}$ direction expand, while the vortices rotating in the opposite direction shrink until they completely vanish (Fig. 3e). Finally, we end up with one pure, stable rotation on $\mathbf{E}_{ext} \times \mathbf{J}$ direction. For isotropic fluid films the scenario shown in Fig. 3a–e is the same. This phenomenon is observed to be independent of the frame geometry.
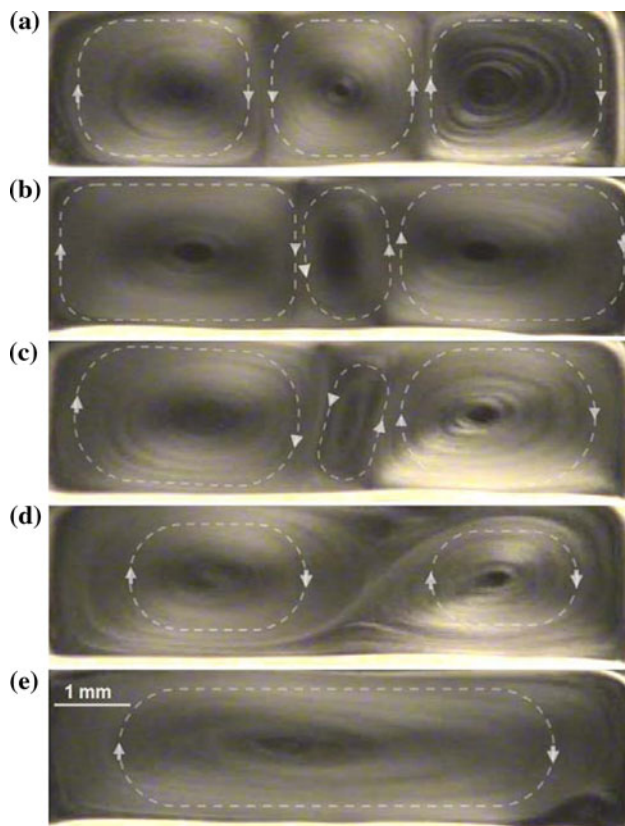

Fig. 3 Experimental observations: applying an external electric field, $\mathbf{E}_{ext}$, on a vortex mode of the MBBA film. While the applied electric voltage, $V_J = 900$ V is kept constant for all cases, and the magnitude of E_{ext} is being changed. **a** $E_{ext} = 0$ kV/m, **b** $E_{ext} = 200$ kV/m, **c** $E_{ext} = 350$ kV/m, **d** $E_{ext} = 450$ kV/m and **e** $E_{ext} = 500$ kV/m

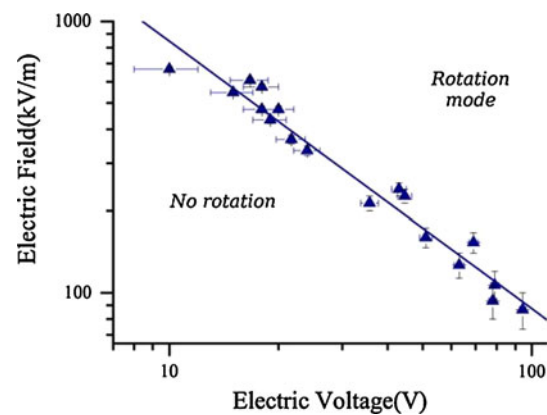**Fig. 4** Threshold of the electric field versus the applied electric voltage for MBBA motion regime, on a frame of (5 × 5 mm)

Applying an electric voltage smaller than the threshold of the vortex mode, does not produce a visible vortices on the film unless a large enough electric field perpendicular to the current is applied. Therefore to have a pure rotation, E_{ext} and V_J are needed to be large enough simultaneously as shown in Fig. 4. Although the thickness of the MBBA and water films differ a lot, similar vortex pattern were observed.

3.2 Pure rotation threshold

The pure rotation thresholds of the MBBA liquid crystal film is studied experimentally by an external electric field $\mathbf{E}_{ext}$ and electric voltage V_J measurements on a square frame of 5 mm × 5 mm. Here, we fix either V_J or E_{ext} and increase the other one until the rotation is observed. The log–log plot of the electric field E_{ext} versus electric voltage V_J) as shown in Fig. 4 indicates a slope of -1.00 ± 0.03. Let us mention that on this plot the scales are logarithmic, and the slope $\Delta y/\Delta x$ is about -1, because $\Delta y = -1{,}000/$
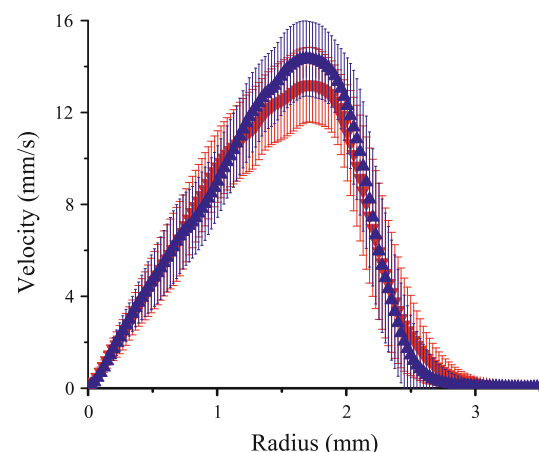

Fig. 5 Velocity versus radius for MBBA film when $V_J = 400$ V and $E_{ext} = 150$ kV/m for isotropic (*blue*) and nematic (*red*) phases

100, and $\Delta x = 100/10$. Thus the experiments indicate that the rotation threshold fields obey simple scaling relation of E_{ext} $V_J = $ Const. This constant value depends on the electric properties and spatial dimensions of the film. The threshold value of $E_{ext} \times V_J = $ Const is obtained from our experiments.

By including some complications, such as considering the leakage currents flowing through the liquid crystal wetting the frame, a mathematical relation could be driven. This graph also shows that as E_{ext} is increased, the required voltage to produce pure rotation decreases significantly.

Fig. 6 The MBBA film at different electric voltages and fields, when the film is placed between two polarizers. The colors on the film indicate that the film motion affects the director direction. **a** Set-up of the experiment. The MBBA film is placed between two perpendicular polarizers to investigate the effect of the rotation, **b** MBBA suspended film just after producing. $E_{ext} = 0$ kV/m and $V_J = 0$ kV, **c** vortices at $E_{ext} = 0$ kV/m and $V_J = 1$ kV, **d** vortices at $E_{ext} = 0$ kV/m and $V_J = 1.2$ kV, **e** vortices at $E_{ext} = 0$ kV/m and $V_J = 1.4$ kV, **f** vortices at $E_{ext} = 0$ kV/m and $V_J = 1.6$ kV, **g** no rotation at $E_{ext} = 300$ kV/m and $V_J = 0$ kV, **h** the film after 20 s. No rotation at $E_{ext} = 300$ kV/m and $V_J = 0$ kV, **i** the film after 100 s. No rotation at $E_{ext} = 300$ kV/m and $V_J = 0$ kV, **j** the film rotation at $E_{ext} = 300$ kV/m and $V_J = 0.5$ kV, **k** increasing the velocity of the rotation. $E_{ext} = 300$ kV/m and $V_J = 1$ kV, **i** expanding the colors on the film. $E_{ext} = 300$ kV/m and $V_J = 1.5$ kV, **m** increasing the velocity. $E_{ext} = 300$ kV/m and $V_J = 2$ kV, **n** reversing the rotation direction. $E_{ext} = 300$ kV/m and $V_J = -2$ kV
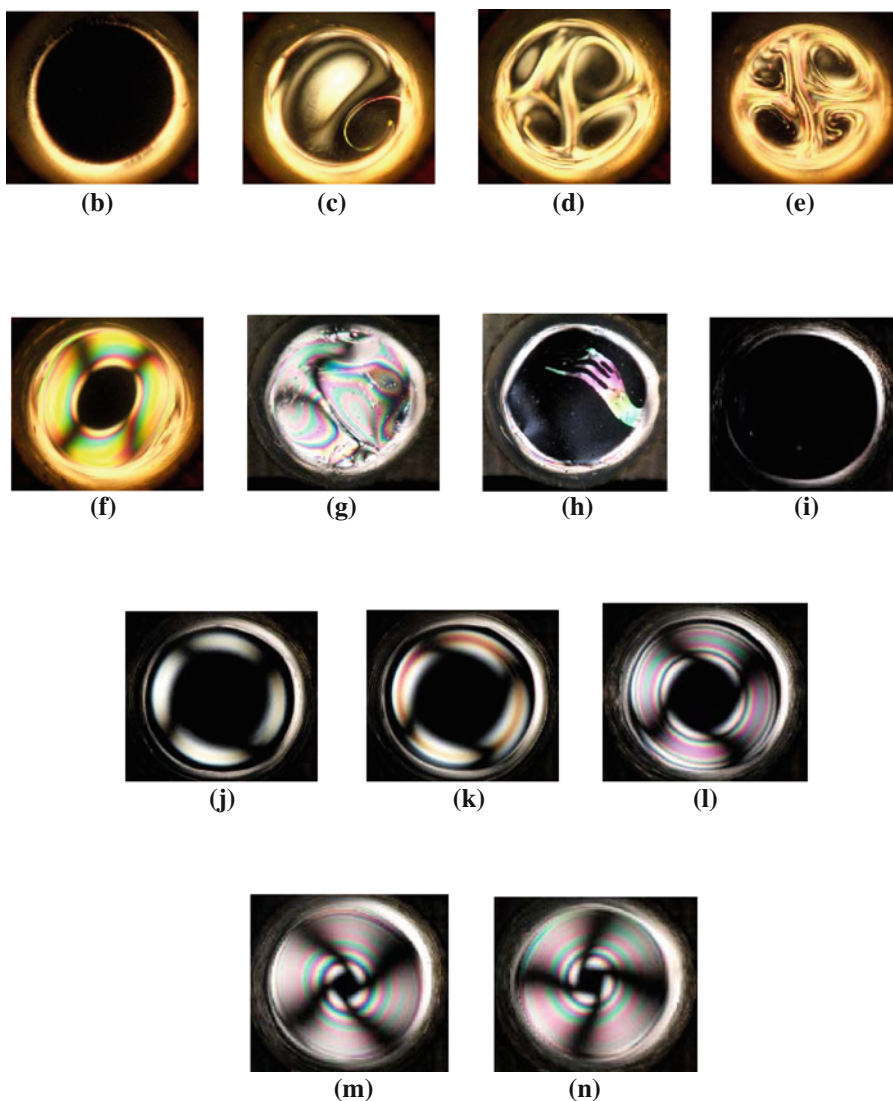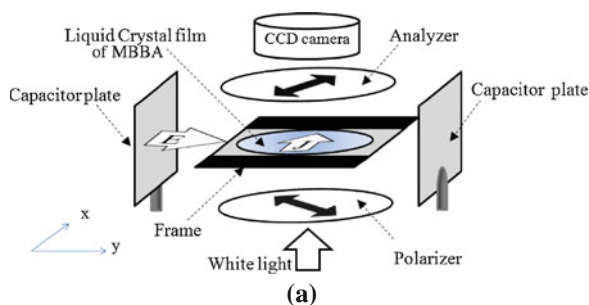
3.3 The angular velocity of rotation

To obtain the angular velocity field of purely rotating MBBA films, particle image velocimetry (PIV) method is used. For a circular frame with a radius of 3.5 mm applied electric field $E_{ext} = 300$ kV/m and current produced by electric voltage $V_J = 2.3$ kV, the rotation shown in Fig. 2a–c is observed. The angular velocity of the MBBA film versus radius is shown in Fig. 2d. This plot for MBBA shows that similar to the case of water films (Amjadi et al. 2009), the angular velocity of MBBA is also a monotonically decreasing function versus radius.

Faetti et al. (1983b) have designed an experiment to show that the EHD vortex patterns in isotropic and anisotropic phases of MBBA suspended films are the same. Our experiments also show that a rotation velocity vector field in isotropic and nematic phases are almost the same as a function of radius shown on (Fig. 5).

3.4 Electro-nematodynamics

Dynamics of a liquid can be studied by Navier–Stokes (NS) and Ericksen–Leslie (EL) equations. In our experiment, the velocity field of the LC film is controllable by electric fields. When NS and EL equations are coupled, the velocity gradient affects the director direction in the MBBA film. Here, we suggest a set-up to observe the electro-nematodynamics effect in MBBA film. To observe this effect, a rotating LC film is placed between two perpendicular polaroids that are parallel to the plane of the film. The phase transition can also be detected by investigating the polarization status of a polarized light beam passing through the film, the results are shown along with the experimental set-up in Fig. 6a. During the experiment, first, E_{ext} was zero (Fig. 6b–f) and the EHD was observed for differend V_Js. Then, the E_{ext} raised to 300 kV/m and kept constant for the rest of the experiment. Then, V_J was varied from zero to 2 kV (Fig. 6g–n) and the rotations were investigated. As shown in Fig. 6g, colors can be observed right after a suspended liquid crystal film is produced. After about 100 s, the colors disappear and the film becomes completely black which implies that the director is perpendicular to the free surface of the film (Fig. 6i). By applying the electric voltage V_J and thus, increasing the velocity of the rotation, colored stripes appear on rotating MBBA film (Fig. 6j–n) gives the pictures of the stable rotation of the LC film. This rotation is based on our experimental observation of tracer particles rotation in LC films. The stripes expand by increasing the electric voltage V_J (Fig. 6j–n). Our observations show that the stripes appear in regions with higher velocities. By increasing the rotation velocity, the stripes expand all over the film except at the center and on the two crossed curved stripes as shown in Fig. 6i. It is clear that the velocity converges to zero at the center of the rotation. The black crossed stripes are the regions in which the projection of the director on the film surface is parallel to one of the polaroids polarization direction. The curvature of the black stripes also depends on the rotation direction. By inverting V_J from 2 to -2 kV rotation direction inverts, and curvature of the strip reverses (Fig. 6m,n; notice that the difference between two cases is only the direction of V_J which could have been the direction of E_{ext}). These evidences imply that the director of liquid crystal at first is perpendicular to the free surface of the film. At the beginning of the film's rotation, the director direction changes and it is no longer remains perpendicular to the film surface, and that is why we see colors on the film. The direction of the director depends on the velocity vector field and the radial symmetry of the colored stripes, which denotes that the velocity vector field has radial symmetry.

4 Conclusion

We have experimentally shown that in freely suspended liquid crystal films of MBBA, the electrohydrodynamic (EHD) vortices convert to a pure rotation in the presence of an additional external electric field. Direction and velocity of the rotation is simply controlled by direction and magnitude of the electric current and the electric field. This rotation is independent of liquid crystal phase of MBBA. Our experiments indicate that the presence of an external electric field helps EHD motions form much easier (with lower voltages) on MBBA liquid crystal films in comparison to the previous studies on EHD.

References

Amjadi A, Shirsavar R, Radja N, Ejtehadi MR (2009) A liquid film motor. Microfluidics Nanofluidics 6:1–5

Atten P (1996) Electrohydrodynamic instability and motion induced by injected space charge in insulating liquids. IEEE Trans Dielectr Electr Insulat 3:1–17

Chandrasekhar S (1992) Liquid crystals. Cambridge University Press, New York

Chomaz JM, Cathalau B (1990) Soap films as two-dimensional classical fluids. Phys Rev A 41:2243–2245

Collins RT, Jones JJ, Harris MT, Basaran OA (2008) Electrohydrodynamic tip streaming and emission of charged drops from liquidcones. Nat Phys 4(2):149–154

Couder Y, Chomaz J, Rabaud M (1989) On the hydrodynamics of soap films. Phys D Nonlinear Phenom 37:384–405

Deyirmenjian VB, Daya ZA, Morris SW (1997) Weakly nonlinear analysis of electroconvection in a suspended fluid film. Phys Rev E Stat Phys Plasmas Fluids Relat Interdiscip Topics 56:1706

Faetti S, Fronzoni L, Rolla PA (1983a) Electrohydrodynamic domain patterns in freely suspended layers of nematic liquid crystals with negative dielectric anisotropy. J Chem Phys 79:5054

Faetti S, Fronzoni L, Rolla PA (1983b) Static and dynamic behavior of the vortex–electrohydrodynamic instability in freely suspended layers of nematic liquid crystals. J Chem Phys 79:1427

de Gennes PG, Prost J (1995) The physics of liquid crystals. Oxford University Press, New York

Grosu FP, Bologa MK (2010) Electroconvective rotation of a dielectric liquid in external electric fields. Surf Eng Appl Electrochem 46(1):43–47

Huang MJ, Wen CY, Lee IC, Tsai CH (2004) Air-damping effects on developing velocity profiles in flowing soap films. Phys Fluids 16:3975–3982

Lee SM, Kang IS (1999) Three-dimensional analysis of the steady-state shape and small-amplitude oscillation of a bubble in uniform and non-uniform electric fields. J Fluid Mech 384:59–91

Lee SM, Im DJ, Kang IS (2000) Circulating flows inside a drop under time-periodic nonuniform electric fields. Phys Fluids 12:1899–1910

Liu Z, Li Y, Zhang G, Jiang S (2011) Dynamical mechanism of the liquid film motor. Phys Rev E Stat Nonlinear Soft Matter Phys 83(2):026303-1–026303-7

Morris SW, Debbuyn JR, May AD (1990) Electroconvection and pattern formation in a suspended smectic film. Phys Rev Lett 65:2378

Ramos A, Morgan H, Green NG, Castellanos A (1998) AC electrokinetics: a review of forces in microelectrode structures. J Phys D Appl Phys 31:2338–2353

Ramos A, Morgan H, Green NG, Castellanos A (1999) AC electric-field-induced fluid flow in microelectrodes. J Colloid Interface Sci 217:420–422

Rivera M, Wu XL (2000) External dissipation in driven two-dimensional turbulence. Phys Rev Lett 85:976–979

Saville DA (1997) Electrohydrodynamics: the Taylor–Melcher leaky dielectric model. Ann Rev Fluid Mech 29:27–64

Shirsavar R, Amjadi A, Tonddast-Navaei A, Ejtehadi MR (2011) Electrically rotating suspended films of polar liquids. Exp Fluids 50:419–428

Shiryaeva EV, Zhukov MY, Vladimirov VA (2009) Rotating electrohydrodynamic flow in a suspended liquid film. Phys Rev E Stat Nonlinear Soft Matter Phys 80:041603-1–041603-15

Sonin AA (1998) Freely suspended liquid crystalline films. Wiley, New York

Xie G, Luo J, Guo D, Liu S (2010a) Nanoconfined ionic liquids under electric fields. Appl Phys Lett 96:043112-1–043112-3

Xie G, Luo J, Liu S, Guo D, Zhang C (2010b) Electric-fields-enhanced destabilization if oil in water emulsionsflowing through acofined wedgelike gap. J Appl Phys 108:064314-1–064314-9

Xie G, Luo J, Liu S, Guo D, Zhang C (2011) Electrospreading of dielectric liquid menisci on the small scale. Soft Matter 7:6076–6081